

## EFFECT OF THE MONOMERS RATIO IN THE ELECTROSYNTHESIS OF POLY(ANILINE-*CO-O*-METHOXYANILINE) ON STEEL CORROSION PROTECTION

M. A. DEL VALLE <sup>a</sup>, F. MIERES <sup>b</sup>, A. MOTHEO <sup>c</sup> AND A. M. R. RAMÍREZ <sup>d\*</sup>

<sup>a</sup>Pontificia Universidad Católica de Chile, Laboratorio de Electroquímica de Polímeros, Av. V. Mackenna 4860, 7820436, Macul, Santiago, Chile.

<sup>b</sup>Ingeniería en Construcción, Facultad de Ciencias, Universidad Mayor, Av. Alemania 0281, 4801043-Temuco, Chile.

<sup>c</sup>Universidade de São Paulo, Instituto de Química de São Carlos, P.O. Box 780, CEP 13560-970, São Carlos, SP, Brasil.

<sup>d</sup>Centro de Nanotecnología Aplicada, Facultad de Ciencias, Universidad Mayor, Av. Alemania 0281, 4801043-Temuco, Chile.

### ABSTRACT

In this work, the synthesis of poly(aniline-*co-o*-methoxyaniline) was carried out on AISI 304 steel, by voltammetric or potentiostatic method. Electropolymerization was achieved from different ratios of 0.4 mol·L<sup>-1</sup> aniline/*o*-methoxyaniline monomers in 1.0 mol·L<sup>-1</sup> H<sub>2</sub>SO<sub>4</sub>. Homo- and copolymers were characterized by cyclic voltammetry, infrared spectroscopy, and scanning electron microscopy. Furthermore, the electrodeposits were studied with a view to their use as corrosion protectors, for which their polarization curve was measured in NaCl 3% and, after 168 h, the surface of the steel was also evaluated by optical microscopy. It was observed that the reactivity that the *o*-methoxy group gives to the aniline ring reduces the protection against corrosion due to the excessive inclusion of N-phenyl-1,4-benzo quinone-di-imine oligomers and/or with an oxazine structure. On the other hand, the optical images confirm the surface damage of the steel, correlating with SEM images that show morphological changes associated with the progress of synthesis and the *o*-methoxy group. Nevertheless, under optimal conditions, poly(aniline-*co-o*-methoxyaniline) modifies the corrosion potential of AISI 304 steel, displacing it by 0.283 V. Furthermore, the presence of small pits and the absence of surface oxide was observed, indicating a significant delay in the oxidation of AISI-304 steel.

**Keywords:** AISI-304 steel; conducting polymer; corrosion; poly(aniline); poly(aniline-*co-o*-methoxyaniline); poly(*o*-methoxyaniline).

### INTRODUCTION

Corrosion implies annual losses close to 3% of the domestic product of a country [1]. This is very difficult to control, especially since there are different types of corrosion, which are classified according to their nature [2]. Also, atmospheric conditions and climate change have clearly strengthened this great problem [3, 4]. This has reinforced the search for new materials, capable of reducing the corrosion rate and increasing the useful life. Among these, steel has been widely used, due to the formation of a protective film, mainly made up of nickel and chromium oxide and hydroxide, which passivates the surface of the material [5, 6]. However, this thin protective layer can be penetrated by compounds based on nitrides, sulfides, and/or chlorides, which produce pitting type corrosion, one of the most common, clearly damaging the useful life of the steel [7].

This has made it necessary to modify the surface of the steel, to reduce its interaction with the environment. Various materials have been used and, among them, conducting polymers (CP) has attracted attention in recent years, due to their redox properties, stability, and the possibility of chemical and electrochemical synthesis [8-10]. And, among CP, the most studied or used for corrosion protection, there is polythiophene (PTh), polypyrrole (PPy) and polyaniline (PAni) [11-14], this last CP being the one that attracts the most attention, due to its low cost, ease of synthesis, high conductivity, greater environmental stability and different redox states, which allow modulating its properties [15]. Thus, this polymer has been tested in the protection against corrosion of various metallic substrates, such as mild steel, stainless steel, iron, aluminum, copper, zinc, among others [11, 16].

On the other hand, the use of copolymers for corrosion protection has also been studied to improve their performance [15, 17], which is explained not only by the mixture of the properties of the monomers used but also by the different morphologies that are achieved when preparing these protective films [18, 19]. Thus, for example, the copolymer of aniline (Ani) and one of its derivatives, *o*-methoxyaniline (OMA), that is, (PAni-*co*-OMA), has shown excellent solubility compared to Ani [20] and, considering that both monomers have good properties for corrosion protection [21]. It was proposed to study its properties in the protection of corrosion in NaCl at 3%. In this case, the authors find that this protective film has lower properties than homopolymers alone [22]. However, the obtaining of this film was carried out by chemical means, with which there is no control of the morphology of the deposit. On the other hand, it has been verified that the electrochemical properties of these materials depend closely on their morphology, which varies depending on experimental variables such as

electrochemical perturbation, concentration, or the type of support electrolyte used during electropolymerization [23-26].

Considering these antecedents, it seems essential to optimize and correlate the morphology of the protective layer with Ani:OMA ratio of PAni-*co*-OMA copolymer, analyzing the effect of concentrations (in this case, the ratio between monomers) and the electrochemical perturbation. This will determine different morphologies of the layer prepared *in situ* and, with this, it will be possible to optimize its effect on the protection against corrosion.

### EXPERIMENTAL

The electropolymerization was carried out in a one-compartment cell, using hydrogen reference electrode (HRE), a platinum wire counter-electrode with an area 20 times greater than that of the working electrode and, as a working electrode, circular AISI 304 steel discs of 1.2 cm in diameter and 0.8 cm thick embedded in polyester resin were used (Figure 1A). Copper wire was employed as an electrical contact. Before use, the electrode was polished and washed manually using granular sandpaper from 100 to 1200. After polishing, they were degreased with ethanol and rinsed with plenty of water and quickly dried.

The modification of the electrodes was carried out from a 0.4 mol·L<sup>-1</sup> total monomer solution of aniline:*o*-methoxyaniline (Ani:OMA) in ratio 1:0; 3:1; 1:1; 1:3, and 0:1 (both monomers being previously double distilled), in 1 mol·L<sup>-1</sup> H<sub>2</sub>SO<sub>4</sub>. It was perturbed by cyclic voltammetry (CV) in a potential interval between 0.05 and 1.15 V, at a potential scan velocity, □□ of 0.05 V·s<sup>-1</sup>, and a number of successive cyclic scans, n = 15, or applying a potential step (FP) of E = 1.15 V during t = 300 s.

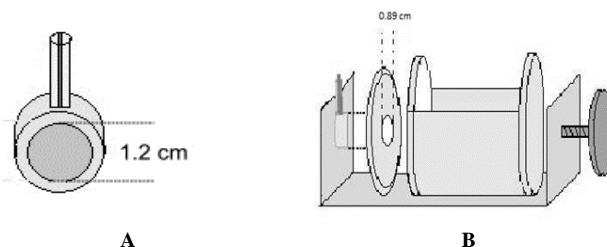


**Figure 1.** Representation of: (A) working electrode, and (B) one-compartment polycarbonate electrochemical cell for corrosion study.

To determine corrosion, a 100 mL one-compartment electrochemical cell (Figure 1B) was used, where the modified electrode was immersed in 3% NaCl during 168 h and the polarization curve recorded at  $\nu = 0.001 \text{ V}\cdot\text{s}^{-1}$ , open circuit potential.

For all electrochemical synthesis and characterization studies a potentiostat/galvanostat Autolab PGSTAT 20 controlled by GPES software was employed. All the experiments were performed at  $25 \pm 2 \text{ }^\circ\text{C}$ , and Milli-Q water was used to prepare solutions and cleaning materials.

Finally, morphology was studied in a scanning electron microscope ZEISS LEICA model DSM 440. To provide an adequate conductivity for the analysis, samples were coated sputtering a nanometric layer of gold.

## RESULTS AND DISCUSSION

Designations of the different electrochemical modified electrodes by CV and FP for the different Ani:OMA ratios are described in Table a.

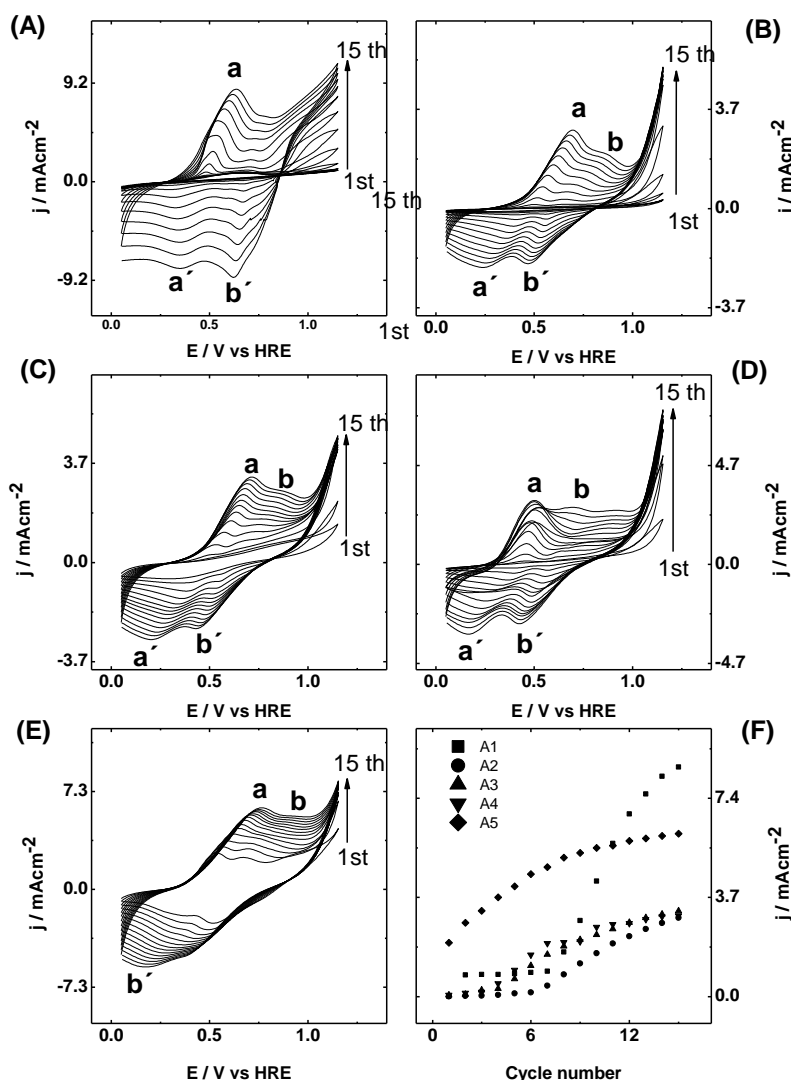
In Figure 2 the cyclic voltammograms corresponding to the surface modifications of AISI 304 steel from the different monomer mixtures between aniline and its derivative are shown. Like polyaniline (Figure 2A), the copolymers present an anodic peak corresponding to the first oxidation of the monomer, characteristic of the transition from leucoemeraldine state to emeraldine salt [27].

**Table a.** Symbology used for samples prepared varying feed for electrosynthesis by cyclic voltammetry (CV) and potential step or fixed potential (FP).

Perturbation	Ratio Ani:OMA	Sample	Perturbation	Ratio Ani:OMA	Sample
CV	1 : 0	A1	FP	1 : 0	B1
	3 : 1	A2		3 : 1	B2
	1 : 1	A3		1 : 1	B3
	1 : 3	A4		1 : 3	B4
	0 : 1	A5		0 : 1	B5

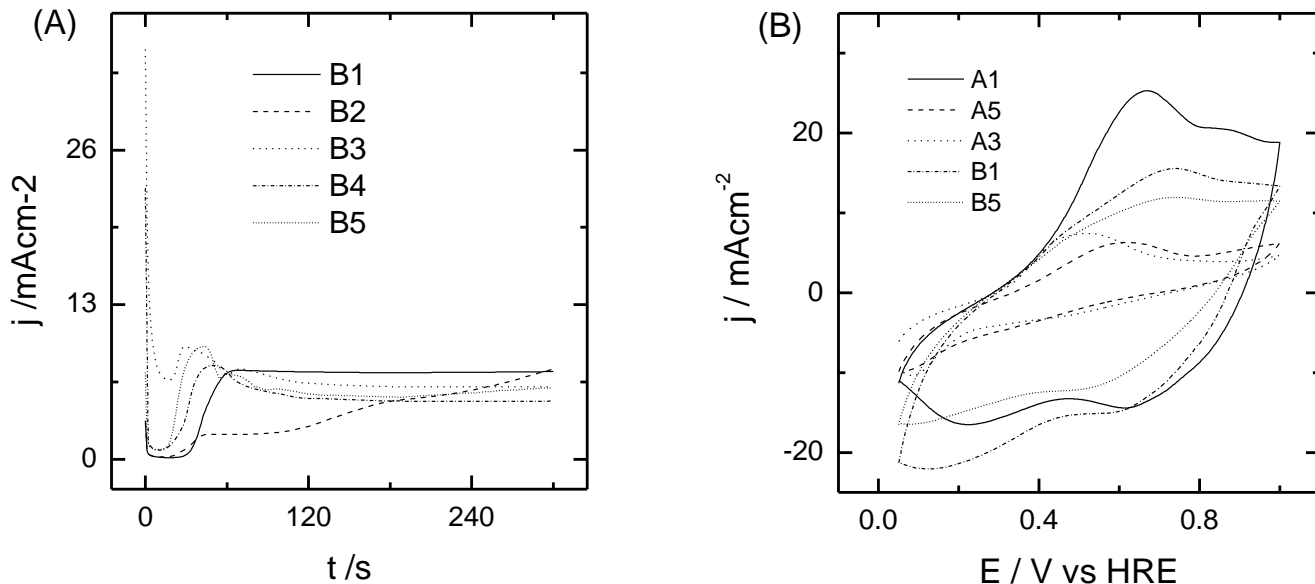
During the electrochemical synthesis of poly-*o*-methoxyaniline (Figure 2E) the anodic currents are much higher than those observed for copolymer synthesis, which is consistent with previously observed results [28]. While, in Figure 2F, peak current vs. cycles number transients are presented, where it is verified that if the concentration of *o*-methoxyaniline in the solution is higher, the growth of the film increases. This is also observed in sample A2, where aniline concentration is three times that of *o*-methoxyaniline. It can be explained considering that the methoxy group increases monomer reactivity.

Figure 3A shows  $j/t$  transients corresponding to the growth of the polymer on the steel surface. In all cases, it is observed that after nucleation, the growth is controlled by diffusion, this situation being more persistent for those having the presence of *o*-methoxyaniline as the starting monomer. This behavior can also be attributed to the increased reactivity provided by the *o*-methoxy substituent.



**Figure 2.** Cyclic voltammograms of AISI 304 steel modified from solution  $0.4 \text{ mol}\cdot\text{L}^{-1}$  monomer and  $1 \text{ mol}\cdot\text{L}^{-1} \text{ H}_2\text{SO}_4$ , according to (A) B1, (B) B2, (C) B3, (D) B4, and (E) B5. (F) Current density,  $j$  vs. cycles number transients of the different modified AISI 304 steel electrodes.

Furthermore, the voltammetric response corresponding to the CV-modified electrodes (Figure 3B) clearly shows that the current density of the copolymer and POMA is lower than that presented by PANi, which can be associated with the conductivity that these films would present. This behavior was also observed for the samples obtained by the potentiostatic method.



**Figure 3.** (A)  $j/t$  transient during the surface modification of AISI 304 steel electrode at FP 1.15 V for 300 s, using the different assayed solutions. (B) Cyclic voltammograms of AISI 304 steel electrodes were modified with the different polymers.

FT-IR spectra were obtained by removing the electrochemically synthesized films from the working electrode and then mixing them with potassium bromide (KBr). These results are shown in Figure 4, where characteristic bands of aniline and its derivatives appear [29]. The CH interaction is observed at 812 and 1111  $\text{cm}^{-1}$  inside and outside the plane, respectively, while the bands corresponding to the C=N stretching were found close to 1573  $\text{cm}^{-1}$ , and around 1298 and 1239  $\text{cm}^{-1}$  the CN stretching of benzenoid rings. Furthermore, the bands corresponding

to the C=C interaction, which are assigned to benzenoid units and quinoid rings, are observed *ca.* 1484  $\text{cm}^{-1}$ . The bands observed at around 1260 and 1120  $\text{cm}^{-1}$ , corresponding to the presence of the methoxy group, intensify as the concentration of *o*-methoxyaniline increases as the starting monomer in the electrolytic solution [30]. Furthermore, the band at 752  $\text{cm}^{-1}$  accounts for the presence of the substitution at position 1,4- [31,32].

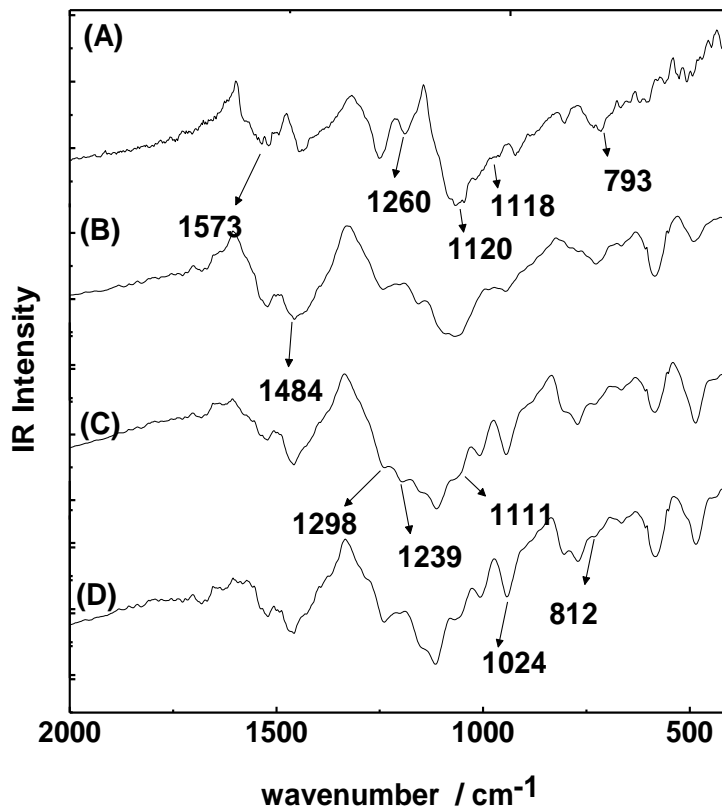


**Figure 4.** FT-IR spectra of the polymers obtained on AISI 304 steel according to (A) A5, (B) A2, (C) B3, and (D) B4.

Figures 5A-C show SEM micrographs of CV-modified electrodes. A compact morphology is seen, which becomes more fibrous as the concentration of *o*-methoxyaniline increases. This is attributable to the fact that the oligomer oxazine, proposed for *o*-anisine, is in the center of the structure, giving preference to this type of growth [33].

On the other hand, the potentiostatically modified electrodes present a granular morphology (Fig. 5D-E), typical in the presence of high acid concentration [34].

Table b shows the data obtained from the potentiodynamic polarization of steel electrodes modified with PANi, POMA, and poly(aniline-*co*-*o*-methoxyaniline) by CV and FP. In all cases, corrosion potentials greater than those presented by bare steel are obtained, as can be verified in Figure 6.

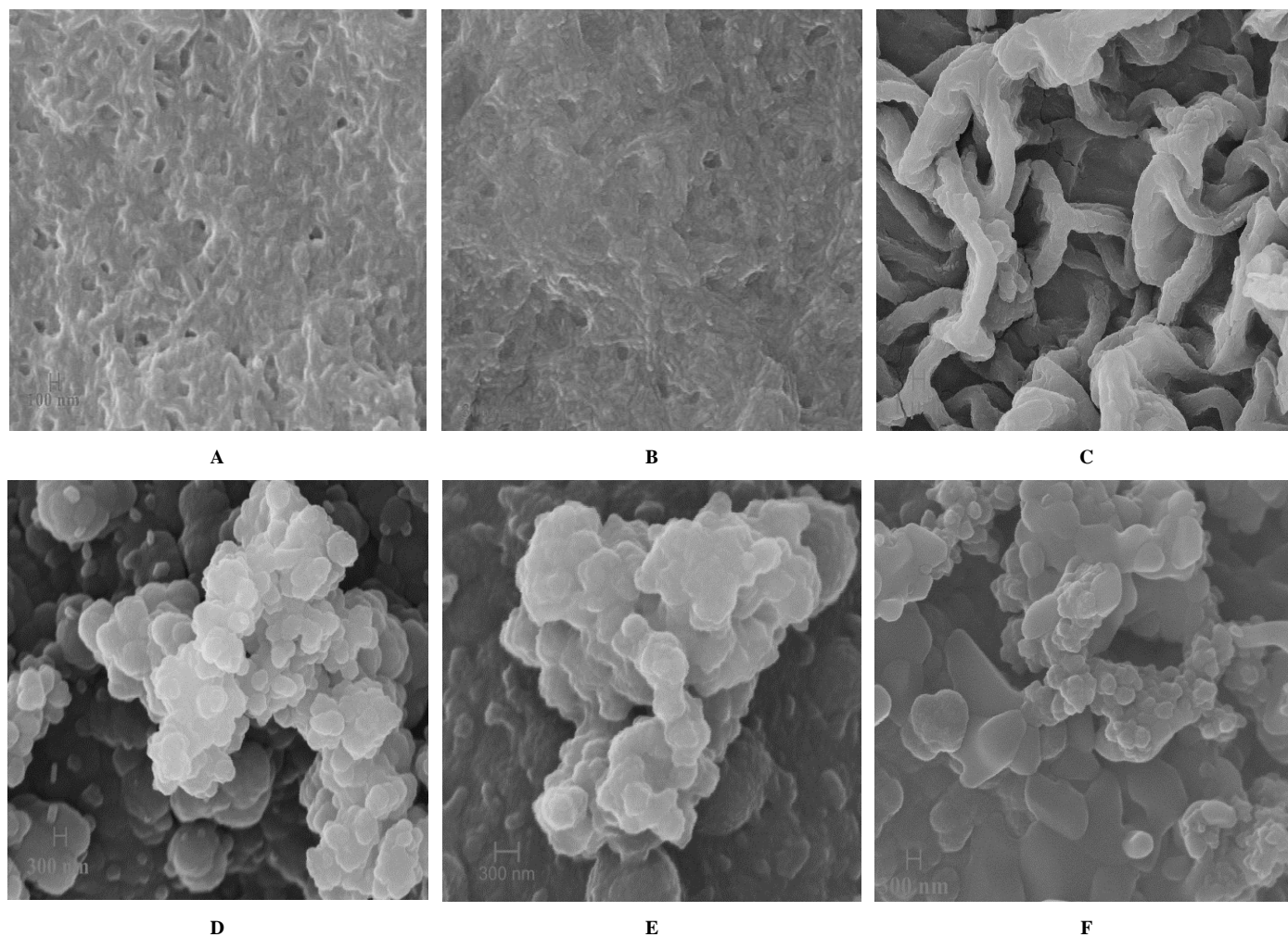


**Figure 5.** SEM micrographs of the deposits obtained according to (A) A1, (B) A2 (B) A5 (D) B1 (E) B2 (F) B5.

**Table b.** Data obtained from the polarization of AISI 304 steel electrodes modified by PANi, POMA, and the copolymer.

Film	$E_c /$ V vs. HRE	$j_c /$ $A \cdot cm^{-2}$	$V_c /$ $mm \cdot year^{-1}$	Film	$E_c /$ V vs. HRE	$j_c /$ $A \cdot cm^{-2}$	$V_c /$ $mm \cdot year^{-1}$
A1	0.176	$1.204 \cdot 10^{-4}$	$1.929 \cdot 10^{-1}$	B1	0.201	$1.162 \cdot 10^{-4}$	$1.86 \cdot 10^{-1}$
A2	0.152	$1.208 \cdot 10^{-5}$	$1.161 \cdot 10^{-2}$	B2	0.243	$9.104 \cdot 10^{-5}$	$1.460 \cdot 10^{-1}$
A3	0.285	$3.014 \cdot 10^{-6}$	$4.040 \cdot 10^{-3}$	B3	0.252	$2.930 \cdot 10^{-5}$	$3.930 \cdot 10^{-2}$
A4	0.206	$1.810 \cdot 10^{-5}$	$2.430 \cdot 10^{-2}$	B4	0.192	$2.118 \cdot 10^{-5}$	$2.840 \cdot 10^{-2}$
A5	0.267	$9.650 \cdot 10^{-5}$	$1.900 \cdot 10^{-3}$	B5	0.214	$7.897 \cdot 10^{-5}$	$1.06 \cdot 10^{-1}$
Steel	0.002	$2.710 \cdot 10^{-6}$	$6.377 \cdot 10^{-3}$				

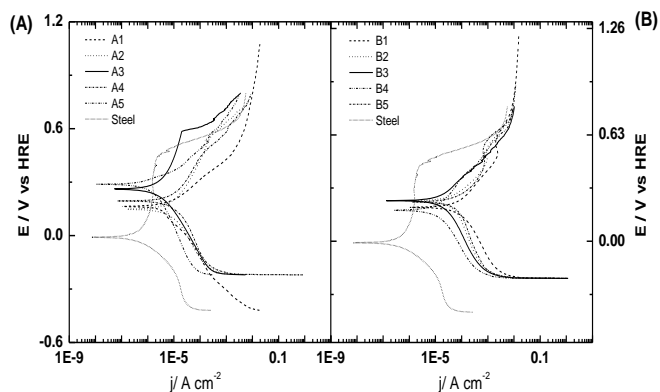


**Figure 6.** Polarization curves of AISI 304 steel electrodes modified by: (A) CV, and (B) FP.

On the other hand, for modifications made by CV, the PANi-*co*-OMA coatings obtained from equal proportions of Ani and OMA (A3), present a greater displacement of the corrosion potential, at more positive values, *ca.* 0.285 V. This behavior can be attributed mainly to the compact morphology, as corroborated by SEM.

This same behavior was observed for the electrodes modified by FP, where sample B3 presents the highest corrosion potentials, which is attributed to the granular morphology that presents this type of modifications, in agreement with that observed in the literature [21, 32, 35, 36]. However, when comparing this sample with A3, the latter shows a greater potential displacement, indicating higher protection against corrosion, because CV allows obtaining the most compact and uniform films.

Additionally, the corrosion current density values obtained are higher than those exhibited by steel, attributable to both polymer degradation and metal dissolution [35]. However, sample A3 presents current density values of the same magnitude as the bare steel, which again is explained by the lower porosity presented by the film prepared in these conditions.

Figure 7 shows the open circuit potentials recorded after immersion of the modified electrodes in 3% NaCl for 168 h (one week). From this, it is observed that the values in the first hour presented quite positive values, clearly indicating their permeability, due to the hydrophobicity of the conducting polymers. On the other hand, samples B2 and B5 have the lowest open circuit potential values, which rapidly decrease in the first hour.

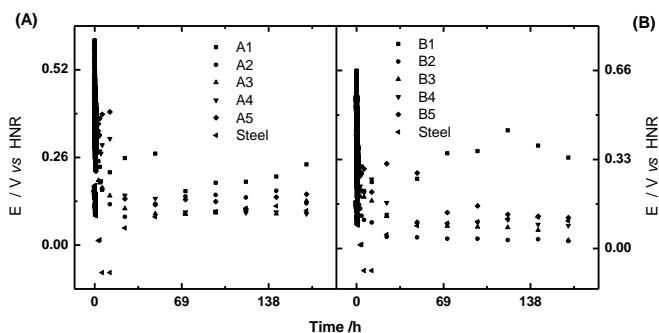


**Figure 7.** Open circuit potential of AISI 304 steel electrodes modified by (A) CV, and (B) FP, and immersed in 3% NaCl for 168 h.

After the first hours of study, the open circuit potential values decrease to values close to those presented by bare steel, to later increase to more positive values, mainly due to the formation of a passive layer on the metal surface.

Figure 8 shows the optical micrographs of the metal surface after 168 h immersed in 3% NaCl. Thus, the exposed steel sample without protection (Figure 8A) presents an oxide film with small black pits, consisting mainly of MnS [7, 37, 38]. In contrast, the steel surface protected by conducting polymer film obtained by CV (Figures 8B-D), the presence of small pits and the absence of surface oxide is observed in all cases, indicating a significant delay in the oxidation of the AISI-304 steel. Likewise, the electrodes modified by fixed potential (Figures 8E-F), present larger pits, indicating greater surface corrosion, attributable to the less compact morphology presented by these polymeric films, as had already been deduced.

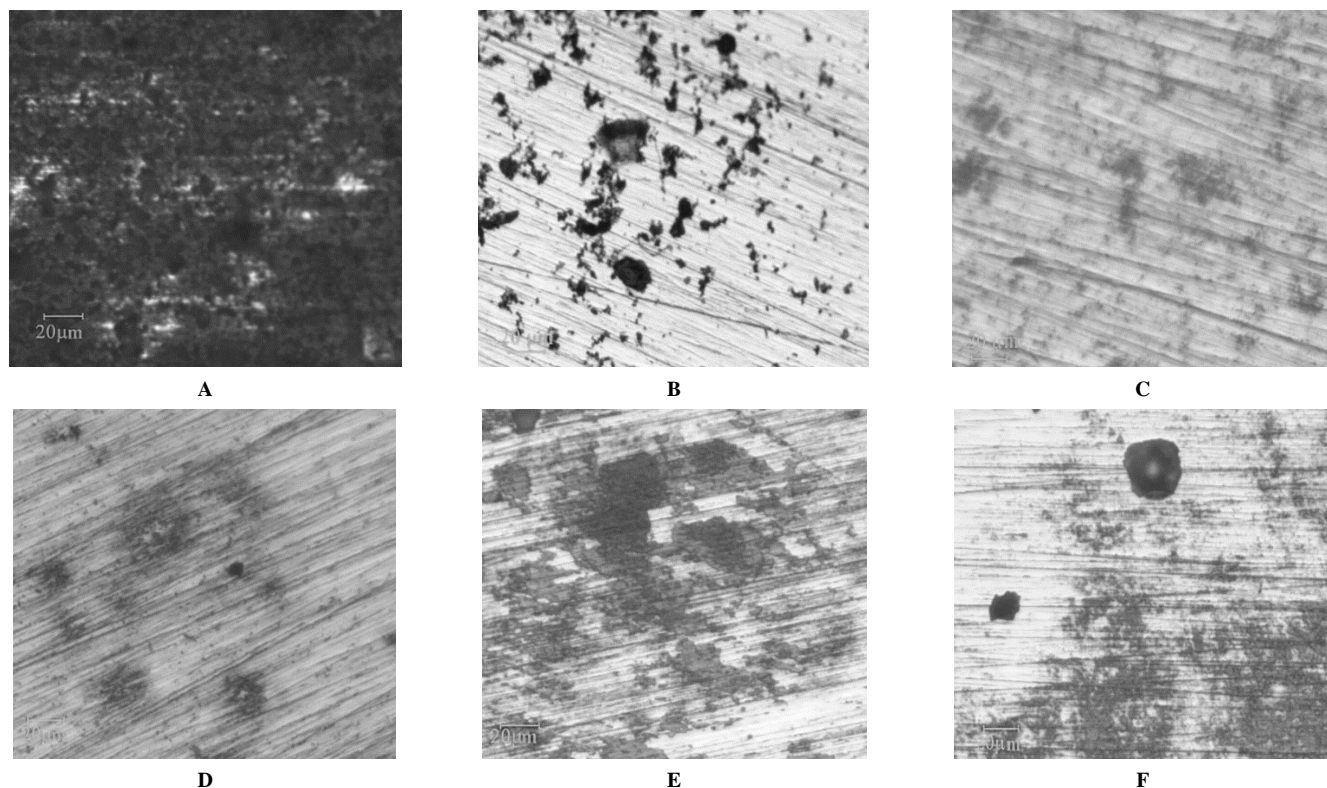


**Figure 8.** Optical micrographs of the AISI 304 steel surface after the immersion of the electrodes in NaCl: (A) bare steel, (B) A1, (C) A3, (D) A5, (E) B3, and (F) B5.

## CONCLUSIONS

The electrosynthesis of poly(aniline-*co-o*-methoxyaniline) on AISI 304 steel by different electrochemical techniques have confirmed that electrochemical perturbation has a strong effect on corrosion protection, cyclic voltammetry being the electropolymerization method that favors the deposit conditions for better protection under these conditions.

On the other hand, the oligomers attributable to the *o*-methoxy group modify the morphology in such a way as to affect the protection against corrosion by the copolymer. Also, the influence of the relationship between aniline and its derivative to form the copolymer on the corrosion protection properties of AISI 304 steel has been demonstrated.

Under optimal conditions, the steel surface protected by poly(aniline-*co-o*-methoxyaniline) obtained by CV modifies the corrosion potential of AISI 304 steel, displacing it by 0.283 V. Moreover, the presence of small pits and the absence of surface oxide is observed, indicating a significant delay in the oxidation of AISI-304 steel. Thus, considering these results, it is possible to propose the next study on the use of this copolymer in biocorrosion in a marine environment, due to the synergistic effect that exists between both homopolymers.

## ACKNOWLEDGEMENTS

The authors acknowledge the financial support of Universidad Mayor I-2019059 and ANID-Chile through Fondecyt 11190995.

## REFERENCES

1. A. Castañeda-Valdéz, M. Rodríguez-Rodríguez, *Revista CENIC Ciencias Químicas*. **45**, 52, (2014).
2. J. A. Salazar-Jimenez, *Tecnol Marcha*. **28**(3), 127, (2015).
3. A. Hernandez, *Rev. Ing. Constr.* **33**(3), 219, (2018).
4. F. Di Turo, C. Proietti, A. Screpanti, M.F. Fornasier, I. Cionni, G. Favero, A. de Marco, *Environ. Pollut.* 218, 586, (2016).
5. R. H. Jung, H. Tsuchiya, S. Fujimoto, *Corros. Sci.* **58**, 62, (2012).
6. I. Ziadi, H. Akrou, H. Hassairi, L. El-Bassi, L. Bousselmi, *Eng. Fail. Anal.* **101**, 342, (2019).
7. P. Schmuki, H. Hildebrand, A. Friedrich, S. Virtanen, *Corros. Sci.* **47**(5), 1239, (2005).
8. M. A. del Valle, A. M. R. Ramirez, L. A. Hernandez, F. Armijo, F. R. Diaz, G. C. Arteaga, *Int. J. Electrochem. Sc.* **11**(8), 7048, (2016).
9. M. A. del Valle, A. M. R. Ramirez, F. R. Diaz, M. A. Pardo, E. Ortega, F. Armijo, *Int. J. Electrochem. Sc.* **13**(12), 12404, (2018).
10. J. F. Pagotto, F. J. Recio, A. J. Motheo, P. Herrasti, *Surf. Coat. Tech.* **289**, 23, (2016).
11. R. Gasparac, C. R. Martin, *J. Electrochem. Soc.* **148**(4), 138, (2001).
12. V. Martina, M. F. de Riccardis, D. Carbone, R. Rotolo, B. Bozzini, C. Mele, *J. Nanopart. Res.* **13**(11), 6035, (2011).
13. J. R. Santos, L. H. C. Mattoso, A. J. Motheo, *Electrochim. Acta.* **43** (3-4), 309, (1998).
14. H. B. Xu, Y. X. Zhang, *Coatings*. **9**(12), 807, (2019).
15. P. P. Deshpande, N. G. Jadhav, V. J. Gelling, D. Sazou, *J. Coat. Technol. Res.* **11**(4), 473, (2014).
16. M. A. Ates, *J. Adhes. Sci. Technol.* **30**(14), 1510, (2016).
17. I. Inamuddin, R. Boddula, M. I. Ahamed, A. M. Asiri, *Polymers Coatings: Technology and Applications*, John Wiley and Sons, hoboken, 2020.
18. G. T. Franco, L. H. E. Santos, C. M. G. S. Cruz, A. J. Motheo, *J. Solid. State. Electr.* **22**(5), 1339, (2018).
19. M. Gao, J. X. Wang, Y. Zhou, P. He, Z. Wang, S. Zhao, *J. Appl. Polym. Sci.* **137**(36), 49049, (2020).
20. L. H. C. Mattoso, L. O. S. Bulhoes, *Synthetic. Met.* **52**(2), 171, 1992.
21. A. T. Ozyilmaz, G. Ozyilmaz, O. Yigitoglu, *Prog. Org. Coat.* **67**(1), 28, (2010).
22. D. Huerta-Vilca, B. Siefert, S. R. Moraes, M. F. Pantoja, A. J. Motheo, *Mol. Cryst. Liq. Cryst.* 415, 229, (2004).
23. R. Schrebler, P. Grez, P. Cury, C. Veas, M. Merino, H. Gomez, R. Córdova, M. A. del Valle, *J. Electroanal. Chem.* **430**(1-2), 77, (1997).
24. A. M. R. Ramirez, M. A. del Valle, F. Armijo, F. R. Diaz, M. A. Pardo, E. Ortega, *J. Appl. Polym. Sci.* **134**(16), 44723, (2017).
25. A. M. R. Ramirez, M. A. Gacitua, E. Ortega, F. R. Diaz, M. A. del Valle, *Electrochem. Commun.* 102, 94, (2019).
26. M. A. del Valle, L. A. Hernandez, A. M. R. Ramirez, F. R. Diaz, *Ionic. Sci.* **23**(1), 191, (2017).
27. D. Sazou, M. Kourouzidou, E. Pavlidou, *Electrochim. Acta.* **52**(13), 4385, (2007).
28. M. A. del Valle, A. Motheo, A. M. R. Ramirez, *J. Chil. Chem. Soc.* **64**(3), 4553, (2019).
29. G. M. Spinks, A. J. Dominis, G. G. Wallace, D. E. Tallman, *J. Solid. State. Electr.* **6**(2), 85, (2002).
30. A. D. Borkar, P. B. Heda, S. S. Umare, *Mater. Res. Innov.* **15**(2), 135, (2011).
31. S. Yalcinkaya, T. Tuken, B. Yazici, M. Erbil, *Prog. Org. Coat.* **62**(2), 236, (2008).
32. S. Chaudhari, A. B. Gaikwad, P. P. Patil, *Curr. Appl. Phys.* **9**(1), 206, (2009).
33. J. Widera, W. Grochala, K. Jackowska, J. Bukowska, *Synthetic Met.* **89**(1), 29, (1997).
34. J. Stejskal, I. Sapurina, M. Trchova, *Prog. Polym. Sci.* **35**(12), 1420, (2010).
35. A. T. Ozyilmaz, N. Colak, G. Ozyilmaz, A. K. Sangun, *Prog. Org. Coat.* **60**(1), 24, (2007).
36. S. M. Ghoreishi, M. Shabani-Nooshabadi, M. Behpour, Y. Jafari, *Prog. Org. Coat.* **74**(3), 502, (2012).
37. D. E. Williams, Y. Y. Zhu, *J. Electrochem. Soc.* **147**(5), 1763, (2000).
38. M. A. Baker, J. E. Castle, *Corros. Sci.* **34**(4), 667, (1993).